

An accurate and real-time ECG noise detection methodology*

D. Nunes, A. Leal, J. Henriques, R. Paiva, P. Carvalho and C. Teixeira

Abstract— The noise contamination of the ECG signals significantly influence the accuracy of algorithms designed to detect several cardiac pathologies such as arrhythmias. Therefore, the existence of reliable noise detection algorithms is crucial.

In this paper we present an algorithm to be used in a pre-processing phase, prior to pathology detection algorithms, by identifying noise periods and by evaluating the ECG signals' quality. The proposed algorithm was designed to detect noisy periods based on single-lead ECG signals. Two main features were considered: the error of the reconstruction by Principal Component Analysis (PCA) and a high frequency feature, the high-pass filtered signal's module.

The algorithm was tested with different noise types, at different SNR levels. With a test set of 49 signals from different leads, comprising approximately 20 hours of recording, the average results were 94.08% and 89.88% of sensitivity and specificity, respectively. The average computational time was 0.14s per 5 minutes of ECG using MATLAB code.

Additionally to the accurate results and low computational cost achieved, the proposed algorithm is robust to different noise types and to the presence of arrhythmia patterns.

I. INTRODUCTION

In an ambulatory acquisition environment the ECG signal may be corrupted by various sources of noise, like electrical activity originated by muscular activity (electromyogram (EMG)), baseline wandering due to the respiration, or even electrode motion, caused mainly by the patient's corporal position changes. The last one presents a predominant prevalence, due to the nature of the acquisition, and the lack of control.

One simple way to deal with noise contaminations lies in discarding the signal segments where those artefacts are identified. In [1], before the separation of sources, a measure of Gaussianity, the negentropy, is used to evaluate the presence of noise segments. In [2], a morphological filtering is performed in order to detect noise segments. The use of accelerometers are explored to detect movement noise in [3]. In [4], statistical metrics are investigated across the first intrinsic mode function (IMF) of an empirical mode decomposition (EMD). In [5], statistical properties are explored on a Laplacian model of the ECG. In [6], the RMS error is computed between the original signal and the approximation resulted from the reconstruction by PCA, using some of the top eigenvectors. In [7], a set of detectors, each one specific to one noise or interference type, is explored. At the end the effects of each interference are weighted to the overall signal quality.

*The Authors are with the Centre for Informatics and Systems, Polo II, University of Coimbra, 3030-290 Coimbra, Portugal {diogo.nunes, adriana.leal}@student.fisica.uc.pt and {jh, ruipedro, carvalho, cteixeir}@dei.uc.pt

In this paper we describe a fast and reliable methodology for noise detection in ECG. This algorithm was designed in order to be integrated in a tele-monitoring system from the WELCOME project (<http://www.welcome-project.eu>), therefore, it was optimized to the characteristics of the referred project, namely ECG's with 5 minutes of duration and sampled at 250 Hz. The noise assessment was performed with consideration of two features: the error of the reconstruction by Principal Component Analysis (PCA) and the high-pass filtered signal's module.

II. MATERIALS AND METHODS

A. Data

Since the referred tele-monitoring system is still in development, we used the ECG signals provided by Physionet (MIT-BIH Arrhythmia Database [8][9]) and noise records from the MIT-BIH Noise Stress Database also from Physionet [10][9], all sampled at 360Hz. Three types of noise were present in these records, the baseline wandering (BW), the EMG artifact (MA), and the electrode motion (EM) artifact. To add noise to the ECG signals at different SNRs, we used the 'nst' function from the WFDB Software Package also provided by Physionet [9], based on a peak-to-peak amplitude to calculate the gains to apply to the noise records. All the signals were resampled to a sampling frequency of 250 Hz.

Based on the overall quality of the signals we extracted a total of 55 ECGs from the entire dataset, 25 of lead II (625 min), 21 of lead V1 (525 min), 4 of lead V2 (100 min), and 5 of lead V5 (125 min). This selection was made to prevent the adverse effect of having noise periods left to annotate, and thus, affecting the algorithm's specificity. Also, with the objective of having a better insight about the algorithm capabilities on detecting different noise types at different SNR's.

The chosen dataset was divided it in two subsets, one for training, and another for testing. We parameterized our algorithm on 6 different signals of lead II, namely the records 201, 205, 213, 217, 223 and 231, comprising a total of 150 minutes. We have chosen this records due to its high quality signal and the presence of various types of arrhythmias, in order to determine the parameters that best discriminate the noise periods, keeping a low sensitivity to arrhythmia patterns.

B. Algorithm

The focus of this algorithm is the detection of noise periods in ECG signals with high adaptation to different leads. It also aims to evaluate the signal's quality depending on the amount and duration of the noise periods. We did not choose a noise reduction strategy since there is a great amount of available ECG data (in a tele-monitoring context),

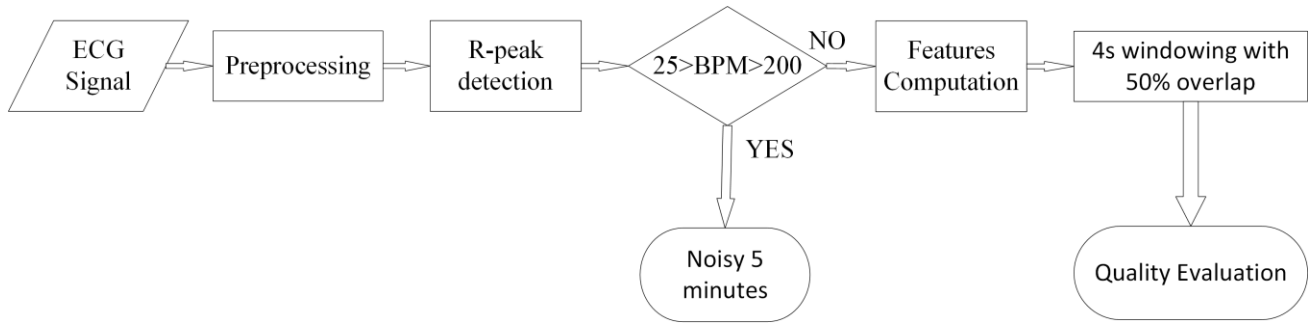


Figure 1. Diagram of the noise detection algorithm in ECG.

and the referred strategy may distort the original signal and lose valuable information.

So we choose to adopt the strategy of removing the noisy periods. The noise detection method comprises four main stages:

- A preprocessing stage where baseline shifts are removed and signal is normalized;
- An R-peak detection stage;
- A feature extraction stage where two features used for classification are computed, namely: the approximation error by PCA [6] and the high-pass filtered signal's module;
- And a final stage where the assessment of noise corruption is performed in 4 seconds windows recurring to the main features.

A diagram that generally depicts the algorithm is shown in Figure 1.

1) Preprocessing:

The algorithm was optimized for 5 minutes segments of ECG signal. If the signal is longer than 5 minutes, the signal is truncated. In each signal, the baseline shifts are removed recurring to a high-pass FIR filtering with a cut-off frequency of 0.5 Hz [11].

2) R-peak detection:

In order to obtain the beat matrix to perform the approximation by PCA, first the ECG is segmented in heartbeats. To do so, we use a R-peak detector based on the Pan & Tompkins algorithm [12]. In order to detect the R-peaks a band-pass filtering between 5 and 20 Hz was implemented. Afterwards, the energy of the signal is derived with the square of its first derivative. The energy is then smoothed by a moving average filter. The modification performed in the Pan & Tompkins algorithm is in the threshold used to assess the peaks locations, which is adaptive. The threshold is derived by the result of a moving average filter with a span of 2 seconds on the resulted energy vector. This modification is made to take in account the different possible beat amplitudes.

Then, a removal of the peaks corresponding to a RR interval lower than 100ms is implemented. As the process of filtering causes a phase shift compared to the original/raw signal, the real peak locations are identified by finding the absolute maximum on the original signal resorting to a back search of 150 ms from the energy peaks locations.

If the rate of beats per minute is below 25 or above 200, the whole 5 min segment is discarded. This is because of the physiological impossibility of this heart rate values, and indicates a disconnection of the electrodes from the skin or a high prevalence of noise.

3) RMS error of the approximation by PCA:

The PCA is performed on the beat matrix (M), which consist in one beat signal per line. Each beat signal B_i in M is obtained from the adjacent R-peaks locations (R_{i-1} and R_{i+1}) of the current R-peak location, R_i (see (1) and (2)).

$$B_i^{\text{reach}} = \min\{(R_i - R_{i-1})/2 ; (R_{i+1} - R_i)/2\} \quad (1)$$

$$B_i = S[k], \quad k = R_i - B_i^{\text{reach}}, \dots, R_i - B_i^{\text{reach}} \quad (2)$$

In (1), B_i^{reach} is the number of samples used to find the extremities of each beat in signal S (see (2)). As the lengths of each beat are different we must perform a resampling to equalize all the beat lengths in order to perform the PCA. The chosen length is 125 samples. All the beats in M suffer a min-max normalization. Then we derive the eigenvalues and the eigenvectors of the covariance matrix of M, and make the reconstruction of the beats matrix based only on the eigenvectors that provide at least 98% of the initial total variance (see (3)). This value was found as the best to discriminate between noise and clean periods according to a ROC analysis.

$$M' = MVV^T \quad (3)$$

In (3), the matrix M' is the result of the reconstruction of M based only on the most significant eigenvectors, V.

$$\text{RMS}_{\text{err}}[i] = \sqrt{\sum_{j=1}^{125} (M'[i, j] - M[i, j])^2} \quad (4)$$

In (4), the vector RMS_{err} is the root mean square error per beat between the original beats and the approximation beats. This vector is one of the features used to assess the presence of noise in ECG segments. Finally, the error sequence is smoothed with a moving average filter.

4) High pass filtered signal's module:

The second feature used to assess the presence of noise is the module of the result of a high-pass 100th order FIR filter with a cut-off frequency of 90 Hz applied to the original ECG (HF_X). The value of 90 Hz corresponds to the best discriminative frequency between noisy and clean periods according to a ROC analysis.

5) *Noise assessment in 4s segments and thresholding:*

The assessment of corrupted periods is done by windowing the whole signal in 4 seconds chunks with 50% of overlap, and by examining the two previously reported features in that time frames. The 4 seconds window was found to have the sufficient length to determine if there is a disconnection of the electrodes based on the beats presence, as also the noise corruption of a given window. Before windowing, thresholds are defined in order to evaluate what is and what is not noise. These thresholds are not fixed to specific values instead they change in each one of the analyzed signals. To set them, we must first look for noise free periods. The clean periods correspond to the 3 segments, each with 10 beats, with minimum RMS_{err} and no overlap. The average error for clean periods, REF_{err} . The thresholds for the first feature are derived from this value as shown in (5) and (6).

$$th1_{err} = f1_{err} \times REF_{err} \quad (5)$$

$$th2_{err} = REF_{err} + f2_{err} \times (th1_{err} - REF_{err}) \quad (6)$$

In (5) and (6), $th1_{err}$ and $th2_{err}$ correspond to the adaptive thresholds for the first feature, RMS_{err} . The constants $f1_{err}$ and $f2_{err}$ were found in the training stage using a ROC analysis and correspond to 2 and 0.5, respectively. To find the thresholds for the second feature, a similar methodology is followed. The same periods of time used to assess REF_{err} are used to calculate the mean value of HF_X , named REF_{HF} (see (7) and (8)).

$$th1_{HF} = f1_{HF} \times REF_{HF} \quad (7)$$

$$th2_{HF} = REF_{HF} + f2_{HF} \times (th1_{HF} - REF_{HF}) \quad (8)$$

$th1_{HF}$ and $th2_{HF}$ correspond to the adaptive thresholds for the second feature, HF_X . In the same way as for $th1_{err}$ and $th2_{err}$, $f1_{HF}$ and $f2_{HF}$ are constants found in the training stage in the ROC curve and correspond to 1.115 and 0.6, respectively.

The reason to choose the RMS_{err} feature to look for clean

periods lies in its highly sensitivity to noise. One may ask, why not just use this feature for classification if it is so sensitive. The reason is that it is also sensitive to uncommon heart beat types, which normally corresponds to abnormal heart beats and rhythms that we want to diagnose. On the other hand, the HF_X feature does not discriminate between different heart beats or rhythm types, even if it has not the noise sensitivity of RMS_{err} . The combination of the two features and the consideration of multiple thresholds provide the algorithm with a more founded decision rule to assess whether a 4s segment signal is noise corrupted or not. Before the final decision rule in (9), in each 4s chunk it is evaluated if there are beats detected by the R-peak detector, if not, the whole chunk is considered as non-quality segment.

$$\text{IF } (\max\{HF_X^w\} > th1_{HF} \ \& \ \max\{RMS_{err}^w\} > th2_{err}) \quad \text{OR} \quad (9)$$

$$(\max\{RMS_{err}^w\} > th1_{err} \ \& \ \max\{HF_X^w\} > th2_{HF})$$

In (9), $\max\{RMS_{err}^w\}$ and $\max\{HF_X^w\}$ represent the maximum values on the 4s window of the first and second features, respectively. If the condition is true, then the whole window is classified as noise corrupted. Figure 2 shows an example of the features' response to a contaminated signal.

III. RESULTS

All the results were computed using MATLAB version R2013b and a 4.00GHz Intel Core i7-4790k processor. To see the influence that different noise types have on a detection algorithm, we tested the corrupted signals at several SNR's.

Based on the results of TABLE I, we consider that the noise influence is only critical in the ranges: [-6, 18] dB for the electrode motion (EM) noise; [-6, 24] dB for the muscle artifact (MA) noise; and [-6, 12] dB for the baseline wandering (BW) noise. The BW noise has less impact at higher SNR levels because this noise type is easily minimized with a detrend operation. ECG detrend is a typical

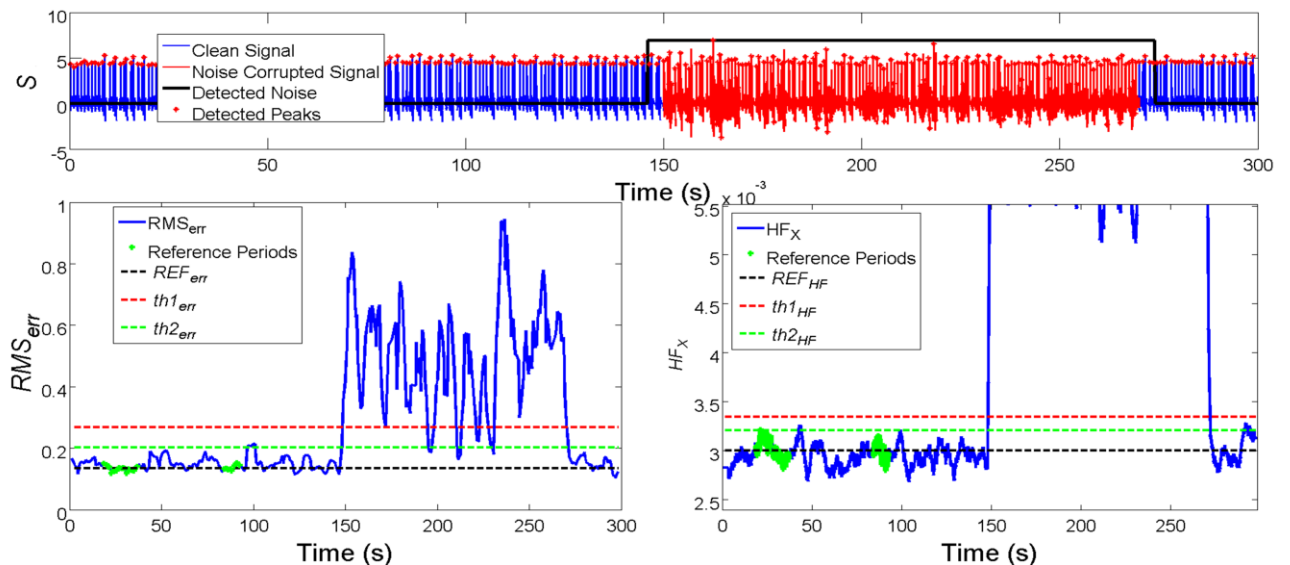


Figure 2- Result of the noise classification performed in an ECG signal with one noise corrupted period.

TABLE I. Results on the influence that different noise types have on the R-peak detector at different SNR levels. These results were computed on the MLII test data. The results on the clean signals were 99.39% and 99.64% of sensitivity (SS) and specificity (SP), respectively.

Noise type	EM		MA		BW	
	SS (%)	SP (%)	SS (%)	SP (%)	SS (%)	SP (%)
-6	36,17	27,41	36,82	34,20	88,86	51,19
0	63,47	43,42	47,48	47,03	95,57	79,24
6	91,28	67,26	63,40	60,70	98,31	92,38
12	98,55	92,30	86,29	73,38	99,26	97,76
18	99,31	98,98	96,90	84,33	99,38	99,34
24	99,37	99,44	99,30	97,36	99,38	99,54

procedure performed by the majority algorithms, thus making BW less troublesome [11].

In the aforementioned noise ranges the results on noise detection where of 94.08% of sensitivity and 89.88% of specificity, as presented in TABLE II.

IV. DISCUSSION

The results in TABLE II show a high sensitivity and specificity in noise detection and also that the accuracy of the algorithm does not vary significantly in different leads, suggesting a good adaptability.

A drawback arising when trying to assess noise contaminated periods in ECG signals relies in the algorithm's possibility to detect abnormal heartbeats or rhythms as noise therefore misclassifying periods with value diagnostic information. It is then essential to evaluate if the false positives are correlated with abnormal heartbeats or rhythms. Our algorithm is capable of a good discrimination between noise and pathological periods, achieving a low sensitivity (below 10%) in the majority of rhythms types, namely atrial fibrillation and flutter, bradycardias, pre-excitation and paced rhythms, as well heart blocks and ventricular bigeminy and trigeminy. The only alarming result in the false positive analysis is the 78.87% detection rate on the supraventricular tachyarrhythmia rhythm in lead MLII, i.e., the developed methodology misclassifies these pathological periods as noise in 78.87% of the times. On the other hand, the whole test dataset only has 14 seconds of this rhythm type in the clean periods, thus so, there is not sufficient statistical size to infer with certainty about the algorithm's sensitivity on this rhythm type.

The highest precision documented in the literature is 96.63% and 94.74% of sensitivity and specificity, respectively, in the ECG noise detection context, recurring to an EMD based algorithm [4]. However, the authors only consider noise corruption in the periods where the R-peaks are not clearly recognizable, indicating that the documented precision is only correspondent for noise corrupted signals at very low SNR levels. Our approach is capable of detecting noise even when the R-peaks are clearly recognizable, suggesting a higher sensitivity to noise. The computational time of the EMD based algorithm is documented in [4] to be 0.2s per 5s of ECG signal at sampling frequency of 180Hz. The computational time of our algorithm is 0.14s per 5 minute ECG signal with a sampling frequency of 250 Hz.

TABLE II. Results for each lead and noise type at critical SNR levels.

	EM		MA		BW		Average per Lead	
	[-6, 18] dB SS	SP	[-6, 24] dB SS	SP	[-6, 12] dB SS	SP	SS	SP
II	97,24	89,92	95,69	90,30	92,84	89,39	95,26	89,87
V1	94,12	88,95	94,71	89,20	96,39	88,68	95,07	88,94
V2	95,86	90,15	94,88	89,57	96,38	88,40	95,71	89,37
V5	90,76	91,60	90,66	90,88	89,39	91,52	90,27	91,33
Avg	94,49	90,16	93,98	89,99	93,75	89,50	94,08	89,88
							TOTAL	

V. CONCLUSION

The noise detection algorithm in ECG demonstrates a high precision and fast performance, as well as a good adaptability for different leads and high specificity even in pathological signals. The results indicate that it is a suitable algorithm to integrate a Tele-monitoring system. Future work will include real-world testing, as also an analysis on the non-tested leads.

ACKNOWLEDGMENT

The authors acknowledge the support of the EU Project WELCOME (FP7 - 611223).

REFERENCES

- [1] H. Yoon, H. Kim, S. Kwon, and K. Park, "An Automated Motion Artifact Removal Algorithm in Electrocardiogram Based on Independent Component Analysis," Fifth Int. Conf. eHealth, Telemedicine, Soc. Med., no. c, pp. 15–20, 2013.
- [2] P. Raphisak, S. C. Schuckers, and A. D. J. Curry, "An algorithm for EMG noise detection in large ECG data," Comput. Cardiol. 2004, vol. 1, no. 1, pp. 369–372, 2004.
- [3] Y. Kishimoto, Y. Kutsuna, and K. Oguri, "Detecting motion artifact ECG noise during sleeping by means of a tri-axis accelerometer," Annu. Int. Conf. IEEE Eng. Med. Biol. - Proc., pp. 2669–2672, 2007.
- [4] J. Lee, D. D. McManus, S. Merchant, and K. H. Chon, "Automatic motion and noise artifact detection in holter ECG data using empirical mode decomposition and statistical approaches," IEEE Trans. Biomed. Eng., vol. 59, no. 6, pp. 1499–1506, 2012.
- [5] A. Mincholé, L. Sörmö, and P. Laguna, "ECG-based detection of body position changes using a Laplacian noise model," Proc. Annu. Int. Conf. IEEE Eng. Med. Biol. Soc. EMBS, vol. 14, pp. 6931–6934, 2011.
- [6] R. Kher, D. Vala, and T. Pawar, "Detection of Low-pass Noise in ECG Signals," no. May, pp. 3–6, 2011.
- [7] I. Jekova, V. Krasteva, I. Christov, and R. Abächerli, "Threshold-based system for noise detection in multilead ECG recordings," Physiol. Meas., vol. 33, no. 9, pp. 1463–1477, 2012.
- [8] G. B. Moody and R. G. Mark, "The impact of the MIT-BIH arrhythmia database," IEEE Eng. Med. Biol. Mag., vol. 20, no. 3, pp. 45–50, 2001.
- [9] A. L. Goldberger, L. A. N. Amaral, L. Glass, J. M. Hausdorff, P. C. Ivanov, R. G. Mark, J. E. Mietus, G. B. Moody, C.-K. Peng, and H. E. Stanley, "PhysioBank, PhysioToolkit, and PhysioNet: Components of a New Research Resource for Complex Physiologic Signals," Circulation, vol. 101, pp. 215–220, 2000.
- [10] G. Moody, W. Muldrow, and R. Mark, "A noise stress test for arrhythmia detectors," in Computers in Cardiology, vol. 11, 1984, pp. 381–384.
- [11] a. B. M. A. Hossain and M. a. Haque, "Analysis of Noise Sensitivity of Different ECG Detection Algorithms," vol. 3, no. 3, 2013.
- [12] J. Pan and W. J. Tompkins, "A real-time QRS detection algorithm," IEEE Trans. Biomed. Eng., vol. 32, no. 3, pp. 230–236, 1985.